Diblock Copolymer Nanospheres with Porous Cores. 2. Porogen Release and Reuptake Kinetics

Guojun Liu* and Jiayun Zhou

Department of Chemistry, University of Calgary, 2500 University Dr., NW, Calgary, Alberta, Canada T2N 1N4

Received April 29, 2002; Revised Manuscript Received July 26, 2002

ABSTRACT: The porogen poly[(2-hydrocinnamoyloxyethyl methacrylate)-*random*-2-(9′-adeninylacetoxyethyl methacrylate), P(hCEMA-*r*-A), and the diblock copolymer poly(*tert*-butyl acrylate)-*block*-poly[(2-cinnamoyloxyethyl methacrylate)-*random*-2-(1′-thyminylacetoxyethyl methacrylate)], P*t*BA-*b*-P(CEMA-*r*-T), formed micelles with P*t*BA coronas and P(CEMA-*r*-T)/P(hCEMA-*r*-A) cores in chloroform/cyclohexane. The cores of the micelles were cross-linked by UV light. Addition of deuterated *N*,*N*-dimethylformamide (DMF-d_7) into a nanosphere solution in deuterated chloroform triggered porogen release. The kinetics was followed by NMR spectroscopy, and a classical model was used to treat the data to yield the diffusion coefficient *D*. The molar mass dependence of *D* suggested that the porogen diffused out of the cores as coils. In neat $CDCl_3$, the porous nanospheres obtained after porogen extraction reuptook the porogen with high efficiency, but the kinetics was more complex than that of porogen release.

I. Introduction

Pores in cross-linked polymer resins can be generated from removing entrapped porogens to enhance reagent transport and to increase internal pore volume and surface areas.[1] Pores have been produced mainly in bulk polymers,[2,3] micrometer-sized beads,[4−6] or monolithic rod columns.[7,8] We reported in the previous paper in this series the generation of pores in the cross-linked cores of diblock copolymer nanospheres.[9] The preparation involved dissolving in chloroform the diblock poly(*tert*-butyl acrylate)-*block*-poly[(2-cinnamoyloxyethyl methacrylate)-*random*-(2-(1′-thyminylacetoxyethyl methacrylate)], P*t*BA-*b*-P(CEMA-*r*-T), and the porogen poly[(2-hydrocinnamoyloxyethyl methacrylate)-*random*-2-(1′-adeninylacetoxyethyl methacrylate), P(hCEMA-*r*-A). The

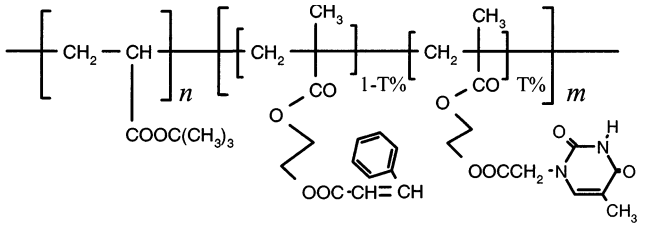

P*t*BA-*b*-P(CEMA-*r*-T)

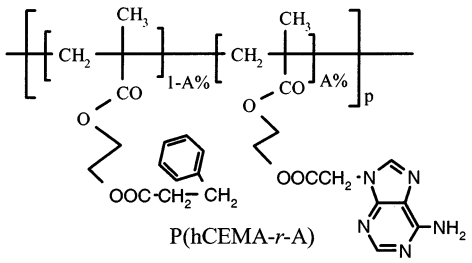

P(hCEMA-*r*-A)

adenine groups (A) in P(hCEMA-*r*-A) and the thymine groups (T) in P*t*BA-*b*-P(CEMA-*r*-T) were probably H-bonded at this stage (Scheme 1). Addition of cyclohexane, which solubilized P*t*BA only, led to the formation of micelles consisting of P(CEMA-*r*-T) and P(hCEMA-*r*-A) cores and P*t*BA coronas. The PCEMA groups in the cores were then photo-cross-linked. Nanospheres with porous cores were obtained after extracting out P(hCEMA-*r*-A). The porous nature of the nanospheres was demonstrated by their much faster uptake of adenine from methanol than the solid nanospheres prepared from P*t*BA-*b*-P(CEMA-*r*-T) without using the porogen. This was also confirmed by the much higher capacity of the porous nanospheres for P(hCEMA-*r*-A) uptake.

The previous paper[9] was concerned with the preparation of the nanospheres and demonstration of their porous nature. The study of fundamental processes such as porogen extraction kinetics was neglected. To show sorbent uptake, we previously separated the porous spheres from the sorbent by a semipermeable membrane. The sorbent, P(hCEMA-*r*-A) or adenine, had to pass the membrane before sorption by the spheres. Without knowing the membrane transport properties, the kinetic data could not be treated quantitatively to deduce sphere properties. We have since found out that the porogen trapped in the nanosphere cores did not show any ^{1}H signals due to excessive peak broadening. NMR has thus been used to follow the kinetics of porogen release from the nanospheres in $CDCl_3$/DMF-d_7 and the kinetics of porogen reuptake by the porous nanospheres from $CDCl_3$. Reported in this paper is the effect of different factors such as molar mass and A-labeling density variation in P(hCEMA-*r*-A) on porogen release and reuptake kinetics.

II. Experimental Section

Polymer Synthesis and Characterization. The PHEMA homopolymer and the P*t*BA-*b*-PHEMA diblock were prepared and characterized following procedures reported in the previous paper.[9] The PHEMA block of the diblock was first cinnamated[10] to yield P*t*BA-*b*-PCEMA, where PCEMA denotes poly(2-cinnamoyloxyethyl methacrylate), before characterization by light scattering, size exclusion chromatography (SEC), and NMR.[11] The specific refractive index increment dn_r/dc of P*t*BA-*b*-PCEMA was determined to be 0.11 mL/g in chloroform. The light scattering molar mass was divided by the polydispersity index from SEC to yield the approximate number-

10.1021/ma020661b CCC: $22.00
Published on Web 09/05/2002

Scheme 1

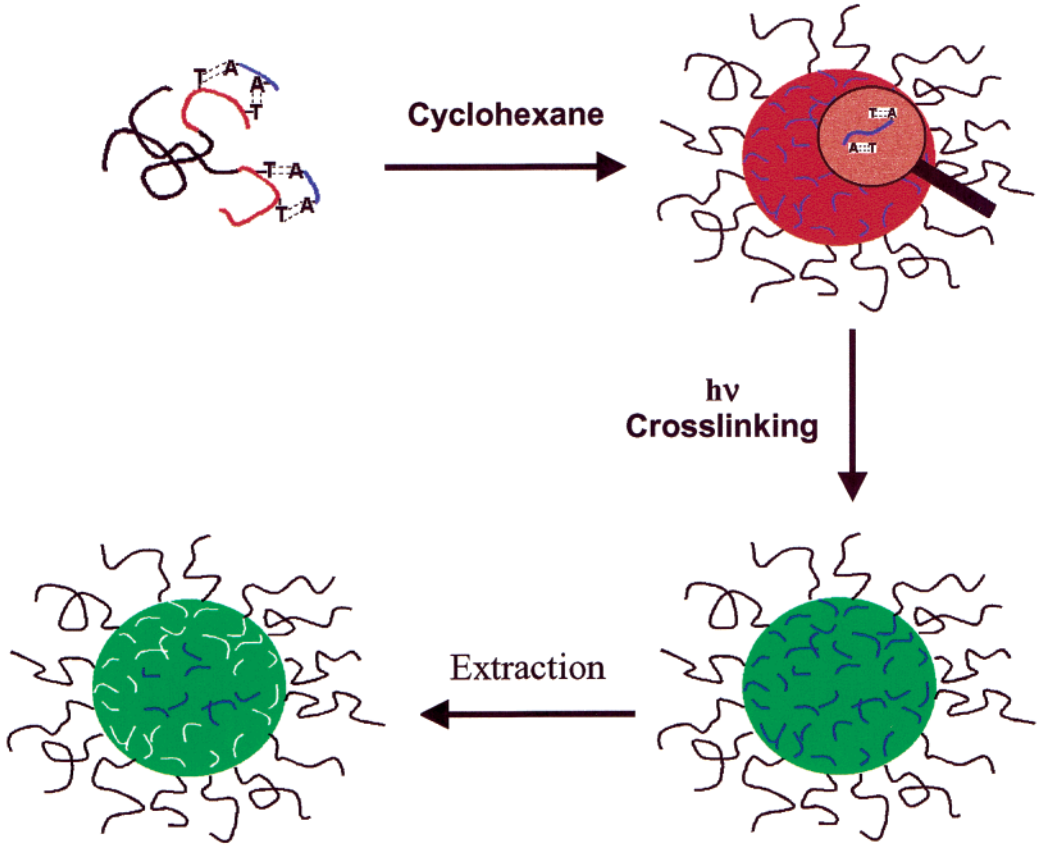

Table 1. Characteristics of the Polymers Used

polymer	dn_r/dc[a] (mL/g)	LS $\bar{M}_w$ [a] (g/mol)	SEC[b] $\bar{M}_n$	SEC[b] $\bar{M}_w/\bar{M}_n$	NMR n/m	$\bar{n}_n$	$\bar{m}_n$	T (%)	A (%)
P*t*BA-*b*-PCEMA	0.11	2.9×10^5	2.2×10^5	1.71	0.93	420	450		
P*t*BA-*b*-P(CEMA-*r*-T)								12	
P(hCEMA-*r*-A)-1			6.3×10^3	1.44					4
P(hCEMA-*r*-A)-2		7.6×10^3	6.3×10^3	1.44					10
P(hCEMA-*r*-A)-3			6.3×10^3	1.44					25
P(hCEMA-*r*-A)-2-F1			6.9×10^3	1.34					9
P(hCEMA-*r*-A)-2-F2			4.8×10^3	1.22					10
P(HEMA-*r*-A)-1									3
P(HEMA-*r*-A)-2									13

[a] Measured in chloroform. [b] Measured in THF.

average molar mass $\bar{M}_n$ for the diblock before the $\bar{M}_n$ value was used with the n/m value determined from NMR to obtain the number-average n and m numbers or the $\bar{n}_n$ and $\bar{m}_n$ values (Table 1). The diblock had a relatively wide distribution but was used anyhow, because the polydispersity did not seem to affect the size distribution of the nanospheres prepared.

The PHEMA sample had ~25 repeat units. It was labeled with adenine groups to yield five P(HEMA-*r*-A) samples with A-labeling molar fractions of 3%, 4%, 10%, 13%, and 25%. The samples with 3% and 13% adenine labeling densities were labeled as P(HEMA-*r*-A)-1 and P(HEMA-*r*-A)-2 and saved for the study of kinetics of P(HEMA-*r*-A) uptake by the porous nanospheres from $CDCl_3/CD_3OD$. The other P(HEMA-*r*-A) samples were reacted with hydrocinnamoyl chloride to yield P(hCEMA-*r*-A) samples. Depending on the adenine group content, the samples were labeled in Table 1 as P(hCEMA-*r*-A)-1, P(hCEMA-*r*-A)-2, and P(hCEMA-*r*-A)-3, respectively. P(hCEMA-*r*-A)-2 with an adenine labeling density of 10% was further separated into two fractions, P(hCEMA-*r*-A)-2-F1 and P(hCEMA-*r*-A)-2-F2, by precipitation fractionation to yield samples with different molar masses but the same A-labeling density. To fractionate the sample, 0.5 g of P(hCEMA-*r*-A)-2 was dissolved in 20 mL of THF first. Slowly added to the solution was then methanol until the mixture just turned turbid. The mixture was left to stand for 4 days at room temperature to yield a two-layer solution with P(hCEMA-*r*-A)-2-F1 in the bottom layer. The dn_r/dc value for P(hCEMA-*r*-A)-2 in toluene was found to be 0.120 mL/g, and the molar mass determined by light scattering was 7.6×10^3 g/mol.

Nanosphere Preparation. The procedure used to prepare nanospheres was similar as that used before.[9,12] Briefly, it involved dissolving 120 mg of P*t*BA-*b*-P(CEMA-*r*-T) with a thymine labeling density of 12% and 40 mg of P(hCEMA-*r*-A)-2, P(hCEMA-*r*-A)-2-F1, or P(hCEMA-*r*-A)-2-F2 in 46 mL of chloroform first. The solution was stirred overnight before 115 mL of cyclohexane was added slowly to induce micelle formation. The formed micelles were then irradiated with UV light that had passed a 290 nm cutoff filter to achieve a CEMA double-bond conversion of 30 ± 1%. Dry nanospheres containing porogen were obtained after rotaevaporating the solvent.

The nanospheres were characterized by transmission electron microscopy (TEM) and dynamic light scattering (DLS) following procedures described previously.[9] A TEM image of such spheres is shown in Figure 1, and the radius for the core averaged over ~100 nanospheres is 15 ± 2 nm. The DLS radius in chloroform is 58 nm.

To obtain porous nanospheres, the irradiated micelle solution was concentrated to ~20 mL and then dialyzed against

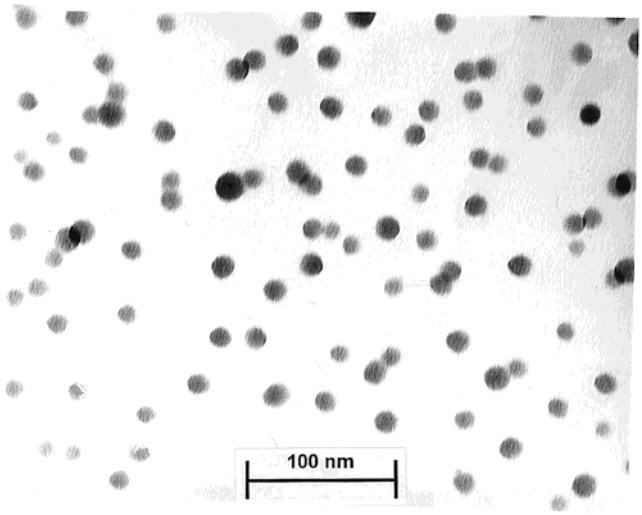

Figure 1. TEM images of P*t*BA-*b*-P(CEMA-*r*-T)/P(hCEMA-*r*-A)-2 nanospheres.

DMF changed six times over 3 days. The dialysis solvent was finally switched to methanol, and the methanol solution of the nanospheres was added onto fresh ice crystals to precipitate out the nanospheres. The nanospheres collected after filtration were dried in vacuo.

P(hCEMA-*r*-A) Release Kinetics. Nanospheres, 15.0 mg, were dissolved in $CDCl_3$. An appropriate amount of DMF-d_7 was then added to achieve the final volume of 0.90 mL and the DMF-d_7 volume fraction of 50% or 67%. The addition of DMF-d_7 triggered porogen release from the core, and ^{1}H NMR analyses were performed to follow the kinetics. Since no magnetic materials were allowed in the tubes during NMR measurement, we did not stir the samples magnetically. Rather, the samples were shaken manually as much as possible throughout the kinetic experiment.

P(hCEMA-*r*-A) or P(HEMA-*r*-A) Uptake. Porous spheres prepared using P(hCEMA-*r*-A)-2 as the porogen were used for all uptake kinetic experiments. Porous spheres, 12.0 mg, and P(hCEMA-*r*-A), 4.5 mg, were each dissolved in 0.45 mL of $CDCl_3$. After their mixing, ^{1}H NMR analyses were performed to follow porogen disappearance from the bulk solution. For studying the kinetics of P(HEMA-*r*-A) uptake, 10.0 mg of the porous nanospheres was dissolved in 0.10 mL of $CDCl_3$ and then mixed with 0.90 or 3.5 mg of P(HEMA-*r*-A) dissolved in 0.50 mL of CD_3OD.

III. Results and Discussion

Porogen Release Kinetic Data. Compared in Figure 2 are the NMR spectra of P*t*BA-*b*-P(CEMA-*r*-T)/P(hCEMA-*r*-A)-2 nanospheres in $CDCl_3$/DMF-d_6 (v/v = 1/2) 15 and 650 min after $CDCl_3$ and DMF-d_6 mixing. Also shown are the peak assignments and an NMR spectrum for P(hCEMA-*r*-A)-2. The porogen signals increased with time.

Shown in Figure 3 is the variation in the amount, $m(t)$, of P(hCEMA-*r*-A)-2 released from the nanospheres as a function of time at DMF-d_7 volume fractions of 50% and 67%, respectively. Increasing DMF-d_7 content increased the porogen release rate due to more efficient competition of DMF-d_7 for H-bonding sites. Shown in Figure 4 are the kinetic data obtained for P(hCEMA-*r*-A)-2-F1 and P(hCEMA-*r*-A)-2-F2 release in $CDCl_3$/DMF-d_7 with 67% DMF-d_7. The release rate is faster for P(hCEMA-*r*-A)-2-F2 with a lower molar mass.

Model of Chain Release Kinetics. As described in the previous paper,[9] the diblock P*t*BA-*b*-P(hCEMA-*r*-T) was derived from P*t*BA-*b*-PHEMA. The T groups were introduced via ester formation between the hydroxyl groups of PHEMA and the carboxyl group of 1-thymine acetic acid and should be randomly distributed in the P(CEMA-*r*-T) block. The A groups, like their binding T groups, and P(hCEMA-*r*-A) should be uni-

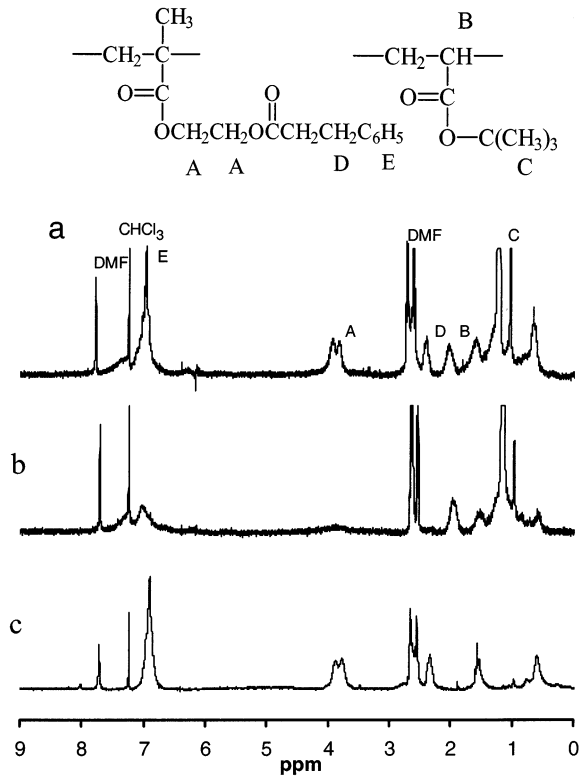

Figure 2. Proton NMR spectra of P*t*BA-*b*-P(CEMA-*r*-T)/P(hCEMA-*r*-A)-2 nanospheres 650 (a) and 15 (b) min after the addition of DMF-d_7 into $CDCl_3$. Spectrum c was obtained for P(hCEMA-*r*-A)-2 alone.

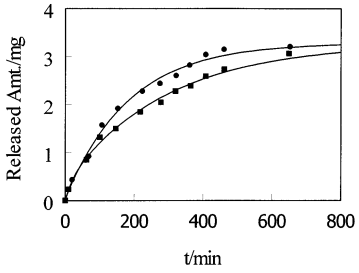

Figure 3. Comparison of the kinetics of P(hCEMA-*r*-A)-2 release from P*t*BA-*b*-P(CEMA-*r*-T)/P(hCEMA-*r*-A)-2 nanospheres in $CDCl_3$/DMF-d_7 at the volume ratios of 1/1 (■) and 1/2 (●). Fifteen milligrams of nanospheres dissolved in a total of 0.90 mL of solvent was used in both of the experiments.

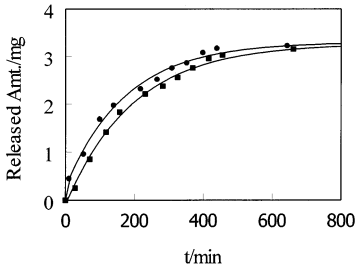

Figure 4. Comparison of P(hCEMA-*r*-A)-2-F1 (■) and P(hCEMA-*r*-A)-2-F2 (●) release kinetics in $CDCl_3$/DMF-d_7 at the volume ratio 1/2. The two samples were cross-linked one after another under identical conditions. Fifteen milligrams of nanospheres dissolved in a total of 0.90 mL of solvent was used in both of the experiments.

Table 2. Parameters Generated from Fitting the P(hCEMA-*r*-A) Release and P(HEMA-*r*-A) Uptake Kinetic Data Using Eq 1

porogen	m_∞	D/R^2 (1/s)	D^a (cm^{-2}/s)	fitting coeff χ^2
	$CDCl_3$/DMF-d_7 at v/v = 1/1			
P(hCEMA-*r*-A)-2	3.39 mg	3.62×10^{-6}	1.45×10^{-17}	0.992
	$CDCl_3$/DMF-$d_7$at v/v = 1/2			
P(hCEMA-*r*-A)-2-F1	3.45 mg	4.76×10^{-6}	1.90×10^{-17}	0.978
P(hCEMA-*r*-A)-2	3.43 mg	5.33×10^{-6}	2.13×10^{-17}	0.983
P(hCEMA-*r*-A)-2-F2	3.40 mg	6.03×10^{-6}	2.41×10^{-17}	0.989
	$CDCl_3/CD_3OD$ at v/v = 1/5			
P(HEMA-*r*-A)-1	34.5 mg/g	16.8×10^{-6}		0.992
P(HEMA-*r*-A)-2	64.9 mg/g	17.2×10^{-6}		0.996

[a] Calculated assuming the swollen core radius of 20 nm.

formly distributed in the cores as well. Then, the spheres were cross-linked in well-stirred solutions, and CEMA cross-linking should be uniform inside a nanosphere core and among different spheres. We further assume that the rate-determining step for the release is the creeping or diffusion of porogen out of the cores, and the size of the cores remains unchanged after porogen release. Based on these considerations and assumptions, the porogen release kinetics should be similar to that of reagent desorption into a well-stirred solution, initially free from solute, from spheres in which the concentration was initially uniform and at c_0.[13]

According to Crank,[13] the amount of reagent desorbed or porogen released, $m(t)$, at time t is

$$m(t) = m_\infty\left(1 - a_1\sum_{i=1}^{\infty}\frac{6\alpha(\alpha+1)\exp(-Dq_n^2t/R^2)}{9+9\alpha+q_n^2\alpha^2}\right) \quad (1)$$

where m_∞ is the amount of porogen released at infinitely long times, D is the diffusion coefficient of the porogen inside the cores, R is the radius of the cores, a_1 is equal to 1 if the infinite series is used but is slightly larger than 1 if the series is truncated in data treatment, and the q_n values at different α values are given in ref 13 and change insignificantly with α for $\alpha > 4$.

The α value in eq 1 is calculated from the final fractional amount retained by the core using

$$\frac{c_0V_{core} - m_\infty}{c_0V_{core}} = \frac{1}{1+\alpha} \quad (2)$$

Figures 3 and 4 show that m_∞ is approximately 3.2 mg. The nanospheres were prepared by mixing 120 mg of P*t*BA-*b*-P(CEMA-*r*-T) with 40 mg of P(hCEMA-*r*-A)-2. Assuming 100% P(hCEMA-*r*-A)-2 incorporation into the nanosphere cores, 15.0 mg of nanospheres should contain 3.75 mg of porogen. The released amount of 3.2 mg was 85% of the theoretical amount. We artificially assumed that the incomplete extraction was due to the porogen partition between the cores and the solvent and obtained from eq 2 $\alpha \approx 5.7$. For this α value, $q_1 = 3.30$, $q_2 = 6.36$, $q_3 = 9.48$, and $q_4 = 12.61$.[13]

We fitted data of Figures 3 and 4 by eq 1 using the first four terms in the series. The fitting coefficients χ^2 (Table 2) are all close to 1, suggesting validity of the diffusion model. To calculate D, we assumed a R value of ~20 nm, which was larger than the TEM radius of 15 ± 2 nm, to account for core swelling by $CDCl_3$/DMF-d_7. The D values (Table 2) show quantitatively that the porogen release rate increased with increasing DMF-d_7 content and decreasing porogen molar mass. Our ability to tune porogen release kinetics by changing the solvation medium, the porogen molar mass, and possibly the porogen molar mass distribution and the cross-linking density of the cores suggests the potential use of this process in controlled drug release.[14]

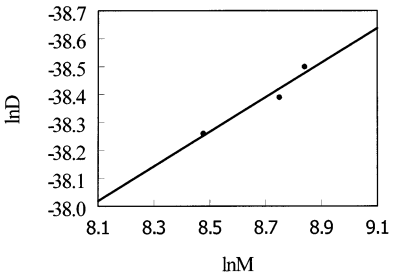

Figure 5. Plot of $\ln[D/(cm^2/s)]$ vs $\ln[\bar{M}_n/(g/mol)]$ for the release of porogens with different molar masses.

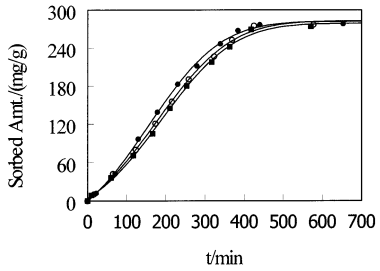

Figure 6. Comparison of kinetics of P(hCEMA-*r*-A)-2-F1 (■), P(hCEMA-*r*-A)-2 (○), and P(hCEMA-*r*-A)-2-F2 (●) uptake by the P*t*BA-*b*-P(CEMA-*r*-T) porous nanospheres in $CDCl_3$. In each experiment, 12.0 mg of porous nanospheres, 4.5 mg of porogen, and 0.90 mL of $CDCl_3$ were used.

The diffusion coefficients of the order of 10^{-17} cm^2/s were low. At 150 °C, Russ et al.[15] measured the diffusion coefficients between 10^{-12} and 10^{-15} cm^2/s for free PS chains with molar masses between 10^4 and 10^5 g/mol in a PS matrix with 0.9% cross-linking density. The D values are much lower here, because the degree of CEMA double-bond conversion was 30%. If half of the CEMA dimerization reactions[16] occurred intermolecularly, the cross-linking density is ~15%. Then, the measurement temperature was much lower in our case.

The D values of P(hCEMA-*r*-A)-2-F1, P(hCEMA-*r*-A)-2, and P(hCEMA-*r*-A)-2-F2 thus determined were plotted in Figure 5 in terms of $\ln(D/(cm^2/s))$ vs $\ln(\bar{M}_n/(g/mol))$, where $\bar{M}_n$ were determined from SEC using poly(methyl methacrylate) as the standards. The slope for the resultant straight line is $-(0.62 \pm 0.15)$, which is the same, within experimental error, as any value between −0.60 and −0.50. A slope between −0.60 and −0.50 suggests that the porogen diffused as coils[17] rather than reptated out of the cores. This is reasonable as the porogen chains were oligomers with lengths probably substantially below the critical entanglement length, which is 173 units for PS.[15] For reptating chains, $D \propto \bar{M}_n^{-2}$.[18]

Kinetics of P(hCEMA-*r*-A) Uptake. The P(hCEMA-*r*-A) chains were sorbed into the cores of the nanospheres again once the solvent was changed to $CDCl_3$. Compared in Figure 6 is the uptake kinetics of porogens of different molar masses. Evidently, the sorption rate increased as the porogen molar mass decreased.

At equilibrium, the amount of porogen sorbed by each gram of porous nanospheres or the capacity was ~280 mg/g. The data of Figures 3 and 4 revealed the extraction of −3.3 mg of porogen from 15.0 mg of P*t*BA-*b*-P(CEMA-*r*-T)/P(hCEMA-*r*-A) spheres or the removal of

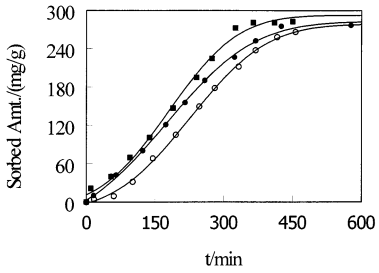

Figure 7. Comparison of P(hCEMA-*r*-A)-3 (■), P(hCEMA-*r*-A)-2 (●), and P(hCEMA-*r*-A)-1 (○) uptake by the P*t*BA-*b*-P(CEMA-*r*-T) porous nanospheres from $CDCl_3$. In each experiment, 12.0 mg of the porous nanospheres, 4.5 mg of porogen, and 0.90 mL of $CDCl_3$ were used.

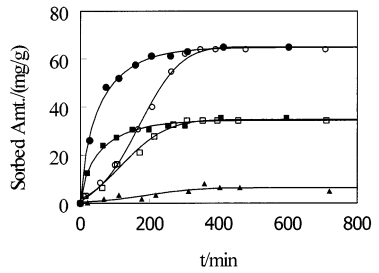

Figure 8. Comparison of the kinetics of P(HEMA-*r*-A) uptake by the P*t*BA-*b*-P(CEMA-*r*-T) porous nanospheres from $CDCl_3$/CD_3OD (v/v = 1/5). In each experiment, 10.0 mg of the porous nanospheres and 0.60 mL of solvent were used. The adenine labeling density in P(HEMA-*r*-A) varied from 0% (▲) to 3% (■ and □) and 13% (○ and ●). The initial P(HEMA-*r*-A) amount was 3.5 mg to obtain the kinetic data denoted by (■) and (●) and 0.90 mg to obtain the other data.

282 mg of porogen from each gram of porous spheres. The agreement between the extracted and sorbed amount suggested the extreme high reutilization efficiency of the pores and the possible retention of the shape and number of cavities inside the cores after porogen extraction.

We have also examined the effect of varying A-labeling density on P(hCEMA-*r*-A) uptake with results shown in Figure 7. While P(hCEMA-*r*-A) uptake rate increased, the nanosphere capacity did not vary much with A-labeling density, suggesting that the pore density governed the capacity. This is reasonable because the PhCEMA chains are structurally close to PCEMA, and a chain can be driven into a cavity probably by the energy of only one T−A binding pair. The rate of sorption increased with increasing A-labeling density, because more T−A binding will make the sorption process more downhill energetically. An energetically more favored process may be faster kinetically as well just as what has been established by Rehm and Weller[19] for many electron-transfer reactions.

We also checked the effect of changing sorbent structure on the reuptake process. Shown in Figure 8 are the data of P(HEMA-*r*-A) uptake by the porous spheres from $CDCl_3$/CD_3OD (v/v = 1/5). As A-labeling density increased, the capacity of the spheres for P(HEMA-*r*-A) increased, as expected. The P(HEMA-*r*-A) sorption rate changed mainly with increasing sorbent concentration.

Unfortunately, P(HEMA-*r*-A) did not dissolve in $CDCl_3$. CD_3OD had H-bonding properties different from $CDCl_3$ and swelled the cross-linked PCEMA cores insignificantly. These differences made the comparison between the uptake data of P(HEMA-*r*-A) and P(hCEMA-*r*-A) difficult.

Model for the Uptake Kinetics. The kinetics of solute sorption and desorption by spheres should be both described by eq 1. We, however, could not treat the data of Figures 6 and 7 by eq 1 to yield reasonable χ^2. The sorbed amount did not increase with time exponentially but had a sigmoidal behavior or followed a S-shaped curve. The same trend is seen in the P(HEMA-*r*-A) sorption data shown in Figure 8 at the P(HEMA-*r*-A) amount of 0.90 mg or the initial concentration of 1.5 mg/mL.

The S-shaped data are normally obtained for the kinetics of bulk free radical polymerization due to the autoacceleration effect.[20] Such curves are also obtained in self-replicating systems, in which the products or offsprings serve as more templates to catalyze reaction.[21] The S-shape thus suggests difficulty in getting a process going. Once a process starts, it accelerates. A logical explanation here is that the initial rate-controlling step is to get the P(hCEMA-*r*-A) chains to penetrate the P*t*BA brush layer on the core surfaces. Once the brush layer is penetrated, subsequent chains may trace the routes of the proceeding ones to keep the supply going. Alternatively, the pore entering step may be rate limiting. This scenario dictates that the chains are adsorbed initially on the surfaces of the cores only via H-binding with the exposed thymine groups. To enter the pores, the adsorbed chains will need to desorb from the surfaces first. Both the desorption and pore entering processes are energetically less favored and can be rate determining.

Brush layers repel polymer chains of the same chemical composition because of the osmotic force derived from the relatively high polymer concentration in the brush.[22] The P*t*BA brush repelled P(HEMA-*r*-A) or P(hCEMA-*r*-A) chains also for their structural dissimilarity. One way to offset this repulsion force is to increase sorbent concentration in the bulk phase. Above a critical concentration, the brush penetration step may not be rate limiting any more, and the sorption kinetics may be described by eq 1 again with $m(t)$ giving the amount sorbed at time t and m_∞ the amount at sorption equilibrium. This seems to explain the concentration dependence of P(HEMA-*r*-A) sorption kinetics shown in Figure 8.

The D/R^2 values generated here (Table 2) are larger than those obtained in $CDCl_3$/DMF-d_7 for P(hCEMA-*r*-A) release probably for the fact that R was smaller in $CDCl_3$/CD_3OD. Then the m_∞ values in $CDCl_3$/CD_3OD as shown in Figure 8 are much lower than the theoretical value of ∼280 mg/g. This suggests a possible nonuniform distribution of the P(HEMA-*r*-A) chains inside the spheres at sorption equilibrium. If the distribution is nonuniform and only the outer layer of the core is penetrated by P(HEMA-*r*-A), the "equivalent" R value or R_e may be even smaller than the sphere radius in $CDCl_3$/CD_3OD. For this ambiguity in R, we did not calculate D in this case.

IV. Conclusions

We have examined the kinetics of P(hCEMA-*r*-A) release from the cross-linked cores of diblock nanospheres into $CDCl_3$/DMF-d_7 and also the kinetics of porogen reuptake by the porous nanospheres from $CDCl_3$. The release kinetics followed a classical model describing reagent diffusion out of spheres into solvent with a finite volume. The molar mass dependence of the porogen diffusion coefficients suggested that the chains

diffused out of the spheres as coils. The porogen re-uptake kinetics was more complex. The penetration of the P*t*BA brush layer on the nanosphere core surfaces might be rate limiting initially. The very slow diffusion of the porogen chains out of the cores could have been monitored here within reasonable time spans mainly due to the small size of the cores. We are currently expanding this method to examine the diffusion of longer polymer chains out of the cores to shed light on chain reptation in cross-linked polymer networks.[15,23]

Acknowledgment. NSERC of Canada is gratefully acknowledged for sponsoring this research. Dr. X. H. Yan prepared Scheme 1, Dr. X. P. Qiu characterized the diblock used by light scattering, Dr. Z. Li synthesized and characterized the PHEMA oligomer, and Dr. F. T. Liu prepared the diblock for another project. Their contributions are gratefully acknowledged.

References and Notes

(1) For reviews on this subject see, for example: (a) Seidl, J.; Malinsky, J.; Dusek, K.; Heitz, W. *Adv. Polym. Sci.* **1967**, *5*, 113. (b) Guyot, A.; Bartholin, M. *Prog. Polym. Sci.* **1982**, *8*, 277.
(2) (a) Wulff, G. *Angew. Chem., Int. Ed. Engl.* **1995**, *34*, 1812. (b) Steinke, J.; Sherrington, D. C.; Dunkin, I. R. *Adv. Polym. Sci.* **1995**, *123*, 81. (c) Shea, K. J. *Trends Polym. Sci.* **1994**, *2*, 166. (d) Sellergren, B. *Angew. Chem., Int. Ed.* **2000**, *39*, 1032.
(3) Zalusky, A. S.; Olayo-Valles, R.; Taylor, C. J.; Hillmyer, M. A. *J. Am. Chem. Soc.* **2001**, *123*, 1519.
(4) Ugelstad, J.; Kaggerud, K. H.; Hansen, F. K.; Berger, A. *Makromol. Chem.* **1979**, *180*, 737.
(5) Wang, Q. C.; Švec, F.; Fréchet, M. J. *J. Polym. Sci., Part A: Polym. Chem.* **1994**, *32*, 2577.
(6) Ye, L.; Mosbach, K. *J. Am. Chem. Soc.* **2001**, *123*, 2901.
(7) Švec, F.; Fréchet, M. J. *Anal. Chem.* **1992**, *64*, 820.
(8) Matsui, J.; Kato, T.; Takeuchi, T.; Suzuki, M.; Yokoyama, K.; Tamiya, E.; Karube, I. *Anal. Chem.* **1993**, *65*, 2223.
(9) Zhou, Y. J.; Li, Z.; Liu, G. J. *Macromolecules* **2002**, *35*, 3690.
(10) Guo, A.; Tao, J.; Liu, G. J. *Macromolecules* **1996**, *29*, 2487.
(11) Tao, J.; Stewart, S.; Liu, G. J.; Yang, M. L. *Macromolecules* **1997**, *30*, 2738.
(12) Henselwood, F.; Liu, G. J. *Macromolecules* **1998**, *31*, 4213.
(13) Crank, J. *The Mathematics of Diffusion*, 2nd ed; Clarendon Press: Oxford, 1975; pp 93−96.
(14) Cammas, S.; Kataoka, K. In *Solvents and Self-Organization of Polymers*; Webber, S. E., Munk, P., Tuzar, Z., Eds.; NATO ASI Series E; Kluwer Academic Publishers: Dordrecht, 1996; Appl. Sci. Vol. 327.
(15) Russ, T.; Brenn, R.; Abel, F.; Boue, F.; Geoghegan, M. *Eur. Phys. J.* **2001**, *E4*, 419.
(16) Guillet, J. E. *Polymer Photophysics and Photochemistry−An Introduction to the Study of Photoprocesses in Macromolecules*; Cambridge University Press: Cambridge, 1985.
(17) See, for example: ter Meer, H.-U.; Burchard, W.; Wunderlich, W. *Colloid Polym. Sci.* **1980**, *258*, 675. The paper presented data showing the molar mass dependence of PMMA diffusion ceofficients in both good and Θ solvents.
(18) De Gennes, P.-G. *Scaling Concepts in Polymer Physics*; Cornell University Press: Ithaca, NY, 1979.
(19) Rehm, D.; Weller, A. *Isr. J. Chem.* **1970**, *8*, 259.
(20) See, for example: Young, R. J.; Lovell, P. A. *Introduction to Polymers*, 2nd ed.; Chapman & Hall: London, 1991.
(21) See, for example: Bachmann, P. A.; Luisi, P. L.; Lang, J. *Nature (London)* **1992**, *357*, 57.
(22) Napper, D. H. *Polymeric Stabilization of Colloidal Dispersions*; Academic Press: London, 1983.
(23) Antonietti, M.; Sillescu, H. *Macromolecules* **1985**, *18*, 1162.

MA020661B